PHYSICAL REVIEW C **82**, 011902(R) (2010)

Transverse momentum dependence of η meson suppression in Au + Au collisions at $\sqrt{s_{NN}} = 200$ GeV

A. Adare,[12] S. Afanasiev,[27] C. Aidala,[40] N. N. Ajitanand,[57] Y. Akiba,[51,52] H. Al-Bataineh,[46] J. Alexander,[57] K. Aoki,[33,51] L. Aphecetche,[59] Y. Aramaki,[11] J. Asai,[51] E. T. Atomssa,[34] R. Averbeck,[58] T. C. Awes,[47] B. Azmoun,[6] V. Babintsev,[23] M. Bai,[5] G. Baksay,[19] L. Baksay,[19] A. Baldisseri,[15] K. N. Barish,[7] P. D. Barnes,[36] B. Bassalleck,[45] A. T. Basye,[1] S. Bathe,[7] S. Batsouli,[47] V. Baublis,[50] C. Baumann,[41] A. Bazilevsky,[6] S. Belikov,[6,*] R. Belmont,[63] R. Bennett,[58] A. Berdnikov,[54] Y. Berdnikov,[54] A. A. Bickley,[12] J. G. Boissevain,[36] J. S. Bok,[66] H. Borel,[15] K. Boyle,[58] M. L. Brooks,[36] H. Buesching,[6] V. Bumazhnov,[23] G. Bunce,[6,52] S. Butsyk,[36] C. M. Camacho,[36] S. Campbell,[58] B. S. Chang,[66] W. C. Chang,[2] J.-L. Charvet,[15] C.-H. Chen,[58] S. Chernichenko,[23] C. Y. Chi,[13] M. Chiu,[6,24] I. J. Choi,[66] R. K. Choudhury,[4] P. Christiansen,[38] T. Chujo,[62] P. Chung,[57] A. Churyn,[23] O. Chvala,[7] V. Cianciolo,[47] Z. Citron,[58] B. A. Cole,[13] M. Connors,[58] P. Constantin,[36] M. Csanád,[17] T. Csörgő,[30] T. Dahms,[58] S. Dairaku,[33,51] I. Danchev,[63] K. Das,[20] A. Datta,[40] G. David,[6] A. Denisov,[23] D. d'Enterria,[34] A. Deshpande,[52,58] E. J. Desmond,[6] O. Dietzsch,[55] A. Dion,[58] M. Donadelli,[55] O. Drapier,[34] A. Drees,[58] K. A. Drees,[5] A. K. Dubey,[65] J. M. Durham,[58] A. Durum,[23] D. Dutta,[4] V. Dzhordzhadze,[7] S. Edwards,[20] Y. V. Efremenko,[47] F. Ellinghaus,[12] T. Engelmore,[13] A. Enokizono,[35] H. En'yo,[51,52] S. Esumi,[62] K. O. Eyser,[7] B. Fadem,[42] D. E. Fields,[45,52] M. Finger Jr.,[8] M. Finger,[8] F. Fleuret,[34] S. L. Fokin,[32] Z. Fraenkel,[65,*] J. E. Frantz,[58] A. Franz,[6] A. D. Frawley,[20] K. Fujiwara,[51] Y. Fukao,[33,51] T. Fusayasu,[44] I. Garishvili,[60] A. Glenn,[12] H. Gong,[58] M. Gonin,[34] J. Gosset,[15] Y. Goto,[51,52] R. Granier de Cassagnac,[34] N. Grau,[13] S. V. Greene,[63] M. Grosse Perdekamp,[24,52] T. Gunji,[11] H.-Å. Gustafsson,[38,*] A. Hadj Henni,[59] J. S. Haggerty,[6] K. I. Hahn,[18] H. Hamagaki,[11] J. Hamblen,[60] J. Hanks,[13] R. Han,[49] E. P. Hartouni,[35] K. Haruna,[22] E. Haslum,[38] R. Hayano,[11] M. Heffner,[35] S. Hegyi,[30] T. K. Hemmick,[58] T. Hester,[7] X. He,[21] J. C. Hill,[26] M. Hohlmann,[19] W. Holzmann,[13,57] K. Homma,[22] B. Hong,[31] T. Horaguchi,[11,22,51,61] D. Hornback,[60] S. Huang,[63] T. Ichihara,[51,52] R. Ichimiya,[51] J. Ide,[42] H. Iinuma,[33,51] Y. Ikeda,[62] K. Imai,[33,51] J. Imrek,[16] M. Inaba,[62] D. Isenhower,[1] M. Ishihara,[51] T. Isobe,[11] M. Issah,[57,63] A. Isupov,[27] D. Ivanischev,[50] B. V. Jacak,[58,†] J. Jia,[6,13,57] J. Jin,[13] B. M. Johnson,[6] K. S. Joo,[43] D. Jouan,[48] D. S. Jumper,[1] F. Kajihara,[11] S. Kametani,[51] N. Kamihara,[52] J. Kamin,[58] J. H. Kang,[66] J. Kapustinsky,[36] K. Karatsu,[33] D. Kawall,[40,52] M. Kawashima,[51,53] A. V. Kazantsev,[32] T. Kempel,[26] A. Khanzadeev,[50] K. M. Kijima,[22] J. Kikuchi,[64] B. I. Kim,[31] D. H. Kim,[43] D. J. Kim,[28,66] E. J. Kim,[9] E. Kim,[56] S. H. Kim,[66] Y. J. Kim,[24] E. Kinney,[12] K. Kiriluk,[12] Á. Kiss,[17] E. Kistenev,[6] J. Klay,[35] C. Klein-Boesing,[41] L. Kochenda,[50] B. Komkov,[50] M. Konno,[62] J. Koster,[24] D. Kotchetkov,[45] A. Kozlov,[65] A. Král,[14] A. Kravitz,[13] G. J. Kunde,[36] K. Kurita,[51,53] M. Kurosawa,[51] M. J. Kweon,[31] Y. Kwon,[60,66] G. S. Kyle,[46] R. Lacey,[57] Y. S. Lai,[13] J. G. Lajoie,[26] D. Layton,[24] A. Lebedev,[26] D. M. Lee,[36] J. Lee,[18] K. B. Lee,[31] K. Lee,[56] K. S. Lee,[31] T. Lee,[56] M. J. Leitch,[36] M. A. L. Leite,[55] E. Leitner,[63] B. Lenzi,[55] P. Liebing,[52] L. A. Linden Levy,[12] T. Liška,[14] A. Litvinenko,[27] H. Liu,[36,46] M. X. Liu,[36] X. Li,[10] B. Love,[63] R. Luechtenborg,[41] D. Lynch,[6] C. F. Maguire,[63] Y. I. Makdisi,[5] A. Malakhov,[27] M. D. Malik,[45] V. I. Manko,[32] E. Mannel,[13] Y. Mao,[49,51] L. Mašek,[8,25] H. Masui,[62] F. Matathias,[13] M. McCumber,[58] P. L. McGaughey,[36] N. Means,[58] B. Meredith,[24] Y. Miake,[62] A. C. Mignerey,[39] P. Mikeš,[8,25] K. Miki,[62] A. Milov,[6] M. Mishra,[3] J. T. Mitchell,[6] A. K. Mohanty,[4] Y. Morino,[11] A. Morreale,[7] D. P. Morrison,[6] T. V. Moukhanova,[32] D. Mukhopadhyay,[63] J. Murata,[51,53] S. Nagamiya,[29] J. L. Nagle,[12] M. Naglis,[65] M. I. Nagy,[17] I. Nakagawa,[51,52] Y. Nakamiya,[22] T. Nakamura,[22,29] K. Nakano,[51,61] J. Newby,[35] M. Nguyen,[58] T. Niita,[62] R. Nouicer,[6] A. S. Nyanin,[32] E. O'Brien,[6] S. X. Oda,[11] C. A. Ogilvie,[26] K. Okada,[52] M. Oka,[62] Y. Onuki,[51] A. Oskarsson,[38] M. Ouchida,[22] K. Ozawa,[11] R. Pak,[6] A. P. T. Palounek,[36] V. Pantuev,[58] V. Papavassiliou,[46] I. H. Park,[18] J. Park,[56] S. K. Park,[31] W. J. Park,[31] S. F. Pate,[46] H. Pei,[26] J.-C. Peng,[24] H. Pereira,[15] V. Peresedov,[27] D. Yu. Peressounko,[32] C. Pinkenburg,[6] R. P. Pisani,[6] M. Proissl,[58] M. L. Purschke,[6] A. K. Purwar,[36] H. Qu,[21] J. Rak,[28,45] A. Rakotozafindrabe,[34] I. Ravinovich,[65] K. F. Read,[47,60] S. Rembeczki,[19] K. Reygers,[41] V. Riabov,[50] Y. Riabov,[50] E. Richardson,[39] D. Roach,[63] G. Roche,[37] S. D. Rolnick,[7] M. Rosati,[26] C. A. Rosen,[12] S. S. E. Rosendahl,[38] P. Rosnet,[37] P. Rukoyatkin,[27] P. Ružička,[25] V. L. Rykov,[51] B. Sahlmueller,[41] N. Saito,[29,33,51,52] T. Sakaguchi,[6] S. Sakai,[62] K. Sakashita,[51,61] V. Samsonov,[50] S. Sano,[11,64] T. Sato,[62] S. Sawada,[29] K. Sedgwick,[7] J. Seele,[12] R. Seidl,[24] A. Yu. Semenov,[26] V. Semenov,[23] R. Seto,[7] D. Sharma,[65] I. Shein,[23] T.-A. Shibata,[51,61] K. Shigaki,[22] M. Shimomura,[62] K. Shoji,[33,51] P. Shukla,[4] A. Sickles,[6] C. L. Silva,[55] D. Silvermyr,[47] C. Silvestre,[15] K. S. Sim,[31] B. K. Singh,[3] C. P. Singh,[3] V. Singh,[3] M. Slunečka,[8] A. Soldatov,[23] R. A. Soltz,[35] W. E. Sondheim,[36] S. P. Sorensen,[60] I. V. Sourikova,[6] N. A. Sparks,[1] F. Staley,[15] P. W. Stankus,[47] E. Stenlund,[38] M. Stepanov,[46] A. Ster,[30] S. P. Stoll,[6] T. Sugitate,[22] C. Suire,[48] A. Sukhanov,[6] J. Sziklai,[30] E. M. Takagui,[55] A. Taketani,[51,52] R. Tanabe,[62] Y. Tanaka,[44] K. Tanida,[33,51,52,56] M. J. Tannenbaum,[6] S. Tarafdar,[3] A. Taranenko,[57] P. Tarján,[16] H. Themann,[58] T. L. Thomas,[45] M. Togawa,[33,51] A. Toia,[58] L. Tomášek,[25] Y. Tomita,[62] H. Torii,[22,51] R. S. Towell,[1] V-N. Tram,[34] I. Tserruya,[65] Y. Tsuchimoto,[22] C. Vale,[6,26] H. Valle,[63] H. W. van Hecke,[36] E. Vazquez-Zambrano,[13] A. Veicht,[24] J. Velkovska,[63] R. Vértesi,[16,30] A. A. Vinogradov,[32] M. Virius,[14] V. Vrba,[25] E. Vznuzdaev,[50] X. R. Wang,[46] D. Watanabe,[22] K. Watanabe,[62] Y. Watanabe,[51,52] F. Wei,[26] R. Wei,[57] J. Wessels,[41] S. N. White,[6] D. Winter,[13] J. P. Wood,[1] C. L. Woody,[6] R. M. Wright,[1] M. Wysocki,[12] W. Xie,[52] Y. L. Yamaguchi,[11,64] K. Yamaura,[22] R. Yang,[24] A. Yanovich,[23] J. Ying,[21] S. Yokkaichi,[51,52] G. R. Young,[47] I. Younus,[45] Z. You,[49] I. E. Yushmanov,[32] W. A. Zajc,[13] O. Zaudtke,[41] C. Zhang,[47] S. Zhou,[10] and L. Zolin[27]

(PHENIX Collaboration)

[1]*Abilene Christian University, Abilene, Texas 79699, USA*

[2]*Institute of Physics, Academia Sinica, Taipei 11529, Taiwan*

[3]*Department of Physics, Banaras Hindu University, Varanasi 221005, India*

[4]*Bhabha Atomic Research Centre, Bombay 400 085, India*
[5]*Collider-Accelerator Department, Brookhaven National Laboratory, Upton, New York 11973-5000, USA*
[6]*Physics Department, Brookhaven National Laboratory, Upton, New York 11973-5000, USA*
[7]*University of California–Riverside, Riverside, California 92521, USA*
[8]*Charles University, Ovocný trh 5, Praha 1, 116 36, Prague, Czech Republic*
[9]*Chonbuk National University, Jeonju 561-756, Korea*
[10]*China Institute of Atomic Energy (CIAE), Beijing, People's Republic of China*
[11]*Center for Nuclear Study, Graduate School of Science, University of Tokyo, 7-3-1 Hongo, Bunkyo, Tokyo 113-0033, Japan*
[12]*University of Colorado, Boulder, Colorado 80309, USA*
[13]*Columbia University, New York, New York 10027 and Nevis Laboratories, Irvington, New York 10533, USA*
[14]*Czech Technical University, Zikova 4, 166 36 Prague 6, Czech Republic*
[15]*Dapnia, CEA Saclay, F-91191, Gif-sur-Yvette, France*
[16]*Debrecen University, H-4010 Debrecen, Egyetem tér 1, Hungary*
[17]*ELTE, Eötvös Loránd University, H-1117 Budapest, Pázmány P. s. 1/A, Hungary*
[18]*Ewha Womans University, Seoul 120-750, Korea*
[19]*Florida Institute of Technology, Melbourne, Florida 32901, USA*
[20]*Florida State University, Tallahassee, Florida 32306, USA*
[21]*Georgia State University, Atlanta, Georgia 30303, USA*
[22]*Hiroshima University, Kagamiyama, Higashi-Hiroshima 739-8526, Japan*
[23]*IHEP Protvino, State Research Center of Russian Federation, Institute for High Energy Physics, Protvino, 142281, Russia*
[24]*University of Illinois at Urbana-Champaign, Urbana, Illinois 61801, USA*
[25]*Institute of Physics, Academy of Sciences of the Czech Republic, Na Slovance 2, 182 21 Prague 8, Czech Republic*
[26]*Iowa State University, Ames, Iowa 50011, USA*
[27]*Joint Institute for Nuclear Research, 141980 Dubna, Moscow Region, Russia*
[28]*Helsinki Institute of Physics and University of Jyväskylä, P.O. Box 35, FI-40014 Jyväskylä, Finland*
[29]*KEK, High Energy Accelerator Research Organization, Tsukuba, Ibaraki 305-0801, Japan*
[30]*KFKI Research Institute for Particle and Nuclear Physics of the Hungarian Academy of Sciences (MTA KFKI RMKI), H-1525 Budapest 114, P.O. Box 49, Budapest, Hungary*
[31]*Korea University, Seoul 136-701, Korea*
[32]*Russian Research Center "Kurchatov Institute", Moscow, Russia*
[33]*Kyoto University, Kyoto 606-8502, Japan*
[34]*Laboratoire Leprince-Ringuet, Ecole Polytechnique, CNRS-IN2P3, Route de Saclay, F-91128, Palaiseau, France*
[35]*Lawrence Livermore National Laboratory, Livermore, California 94550, USA*
[36]*Los Alamos National Laboratory, Los Alamos, New Mexico 87545, USA*
[37]*LPC, Université Blaise Pascal, CNRS-IN2P3, Clermont-Fd, 63177 Aubiere Cedex, France*
[38]*Department of Physics, Lund University, Box 118, SE-221 00 Lund, Sweden*
[39]*University of Maryland, College Park, Maryland 20742, USA*
[40]*Department of Physics, University of Massachusetts, Amherst, Massachusetts 01003-9337, USA*
[41]*Institut fur Kernphysik, University of Muenster, D-48149 Muenster, Germany*
[42]*Muhlenberg College, Allentown, Pennsylvania 18104-5586, USA*
[43]*Myongji University, Yongin, Kyonggido 449-728, Korea*
[44]*Nagasaki Institute of Applied Science, Nagasaki-shi, Nagasaki 851-0193, Japan*
[45]*University of New Mexico, Albuquerque, New Mexico 87131, USA*
[46]*New Mexico State University, Las Cruces, New Mexico 88003, USA*
[47]*Oak Ridge National Laboratory, Oak Ridge, Tennessee 37831, USA*
[48]*IPN-Orsay, Universite Paris Sud, CNRS-IN2P3, BP1, F-91406, Orsay, France*
[49]*Peking University, Beijing, People's Republic of China*
[50]*PNPI, Petersburg Nuclear Physics Institute, Gatchina, Leningrad region, 188300, Russia*
[51]*RIKEN Nishina Center for Accelerator-Based Science, Wako, Saitama 351-0198, Japan*
[52]*RIKEN BNL Research Center, Brookhaven National Laboratory, Upton, New York 11973-5000, USA*
[53]*Physics Department, Rikkyo University, 3-34-1 Nishi-Ikebukuro, Toshima, Tokyo 171-8501, Japan*
[54]*Saint Petersburg State Polytechnic University, St. Petersburg, Russia*
[55]*Universidade de São Paulo, Instituto de Física, Caixa Postal 66318, São Paulo CEP 05315-970, Brazil*
[56]*Seoul National University, Seoul 151-742, Korea*
[57]*Chemistry Department, Stony Brook University, SUNY, Stony Brook, New York 11794-3400, USA*
[58]*Department of Physics and Astronomy, Stony Brook University, SUNY, Stony Brook, New York 11794, USA*
[59]*SUBATECH (Ecole des Mines de Nantes, CNRS-IN2P3, Université de Nantes) Boîte Postale 20722-44307, Nantes, France*
[60]*University of Tennessee, Knoxville, Tennessee 37996, USA*
[61]*Department of Physics, Tokyo Institute of Technology, Oh-okayama, Meguro, Tokyo 152-8551, Japan*
[62]*Institute of Physics, University of Tsukuba, Tsukuba, Ibaraki 305, Japan*

[63] *Vanderbilt University, Nashville, Tennessee 37235, USA*
[64] *Waseda University, Advanced Research Institute for Science and Engineering, 17 Kikui-cho, Shinjuku-ku, Tokyo 162-0044, Japan*
[65] *Weizmann Institute, Rehovot 76100, Israel*
[66] *Yonsei University, IPAP, Seoul 120-749, Korea*
(Received 26 May 2010; published 27 July 2010)

New measurements by the PHENIX experiment at the Relativistic Heavy Ion Collider for η production at midrapidity as a function of transverse momentum (p_T) and collision centrality in $\sqrt{s_{NN}} = 200$ GeV Au + Au and $p + p$ collisions are presented. They indicate nuclear modification factors ($R_{\rm AA}$) which are similar in both magnitude and trend to those found in earlier π^0 measurements. Linear fits to $R_{\rm AA}$ as a function of p_T in 5–20 GeV/c show that the slope is consistent with zero within two standard deviations at all centralities, although a slow rise cannot be excluded. Having different statistical and systematic uncertainties, the π^0 and η measurements are complementary at high p_T; thus, along with the extended p_T range of these data they can provide additional constraints for theoretical modeling and the extraction of transport properties.

DOI: 10.1103/PhysRevC.82.011902 PACS number(s): 25.75.Dw, 13.85.Qk, 13.20.Fc, 13.20.He

Suppression of high-p_T hadron production in Au + Au collisions at the Relativistic Heavy Ion Collider (RHIC) [1,2] and its absence in d + Au collisions [3] provided the first direct evidence that an extremely dense medium is formed in heavy ion collisions at RHIC energies. This suppression relative to the yield expected from the convolution of independent nucleon-nucleon scatterings, measured by the nuclear modification factor $R_{\rm AA}$, is now confirmed up to 20 GeV/c with identified π^0 and attributed to the energy loss of the hard scattered partons in the dense medium. Several models with very different assumptions describe the magnitude of the observed π^0 suppression, but predict slightly different evolution with increasing p_T. Calculations based on perturbative quantum chromodynamics (pQCD) and static plasma predict that the fractional parton energy loss decreases with p_T as $\log(p_T)/p_T$, leading to a slow rise of the $R_{\rm AA}$ with p_T (for a recent review see [4]). In contrast, some anti–de Sitter Conformal Field Theory (CFT) calculations find that the fractional energy loss is proportional to p_T. Therefore, $R_{\rm AA}$ *decreases* with increasing transverse momentum [5–8]. The universal upper bound model [9] predicts that $R_{\rm AA}$ remains almost independent of the energy of the original gluon or quark. Other effects (modified nuclear parton distribution functions, Cronin effect, modified fragmentation functions, and the quark/gluon ratio) at given x_T ($2p_T/\sqrt{s}$) can also change the p_T dependence of $R_{\rm AA}$. A precise measurement of the evolution of $R_{\rm AA}$ with p_T would help in confirming or rejecting classes of theories and putting tight constraints on the free parameters of the remaining ones. The first rigorous attempt to confront the observed π^0 suppression with various pQCD-based parton energy loss calculations and to put quantitative constraints on the transport properties of the medium was made in [10] using PHENIX π^0 data. One intriguing result was that a linear fit with a slope consistent with zero described the evolution of $R_{\rm AA}$ with p_T slightly better than any of the pQCD models predicting a slow rise. However, the large statistical and systematic uncertainties of the high-p_T π^0 points prevented a clear distinction between constant or slowly rising $R_{\rm AA}$.

One reason the π^0 data [2] allow such ambiguous interpretations is that the experimental uncertainties rise rapidly as we move to higher p_T (>12–14 GeV/c), because of "shower merging," as explained below. In the case of the η this problem is absent for p_T up to 50 GeV/c, significantly beyond the p_T range expected to be accessible at RHIC. While the yield of the actually reconstructed η mesons is smaller except at the highest p_T, the improvement in systematic uncertainties can help provide better constraints in comparisons to theory at high p_T and thus complement the π^0 results. Of course, some caution in interpreting the results is warranted: while both π^0 and η consist of light quarks, η does have a hidden strangeness ($s\bar{s}$) content so it is not *a priori* obvious that the π^0 and η results are interchangeable. Earlier measurements [11] have shown that, at least up to 12 GeV/c, the π^0 and η nuclear modification factors in Au + Au agree within uncertainties and the η/π^0 ratio is constant for $p_T \geqslant 4$ GeV/c in $p + p$ [11]. Using recent, more precise measurements in PHENIX, we will reexamine whether π^0 and η production at midrapidity is indeed similar and study the asymptotic behavior of $R_{\rm AA}$.

This analysis used 3.25B minimum bias (MB) $\sqrt{s_{NN}} =$ 200 GeV Au + Au events, corresponding to 0.511 nb^{-1} recorded in 2007 as well as 429M minimum bias (18.7 nb^{-1}) and 2.06B triggered (6.90 pb^{-1}) $\sqrt{s} = 200$ GeV $p + p$ events recorded in 2006 in the PHENIX experiment at RHIC. Both the Au + Au and $p + p$ data sets were analyzed using the same analysis chain and cuts; thus, some of the systematic uncertainties cancel when we calculate the nuclear modification factor $R_{\rm AA}$ for Au + Au. Collision centrality in Au + Au has been established by the beam-beam counters (BBCs, $3.0 < |\eta| < 3.9$) [12]. A Glauber-model Monte Carlo [13] along with a simulation of the BBC response was used to estimate the average number of participating nucleons ($N_{\rm part}$) and binary nucleon-nucleon collisions ($N_{\rm coll}$) for each centrality bin.

The η mesons were measured via their $\eta \to \gamma\gamma$ decay channel. The photons were reconstructed in the lead-scintillator (PbSc) sectors of the PHENIX electromagnetic calorimeter (EMCal) [14] covering 3/8 of the full azimuth and $-0.35 < \eta < 0.35$ in pseudorapidity, and the η yield was extracted from

*Deceased.
†PHENIX spokesperson; jacak@skipper.physics.sunysb.edu

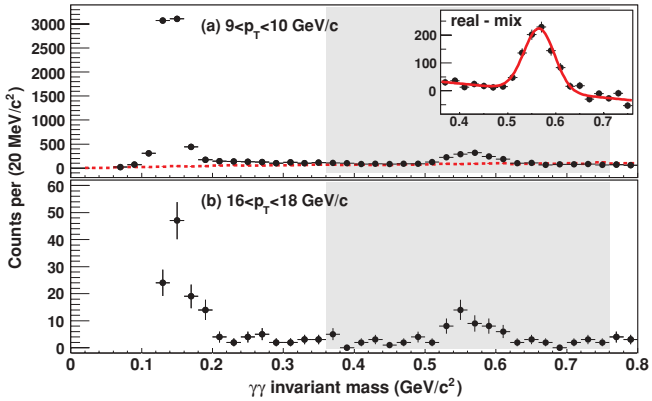

FIG. 1. (Color online) $\gamma\gamma$ invariant mass distribution for two different bins in p_T of the $\gamma\gamma$ pair (minimum bias data). (a) $9 < p_T < 10$ GeV/c, both foreground (real, points) and normalized combinatorial background (mix, dashed lines) are shown. Note the large difference between π^0 and η raw yields. Inset: the magnified η region after background subtraction. (b) $16 < p_T < 18$ GeV/c region, where mixed event subtraction is no longer necessary. Also, here a cut on the γ-pair energy asymmetry, $\alpha < 0.6$, has been applied, which greatly improves the signal-to-background ratio at the η peak but cuts into the lower part of the π^0 peak owing to cluster merging.

two-photon invariant mass distributions. There are important differences between π^0 and η measurements. In the case of π^0, starting around $p_T = 12$ GeV/c the minimum opening angle of the two decay photons is small enough for the photon showers to merge and become indistinguishable. As p_T increases, this effect leads to an increasing loss of observed π^0, resulting in large corrections and corresponding systematic uncertainties (which are in fact the dominant systematic uncertainties at high p_T). Since the mass of the η is about four times larger than the π^0, this is not a problem for the η measurement up to $p_T \sim 50$ GeV/c. However, the observable η rates are much lower at low and medium p_T, as seen in the invariant mass distributions in Fig. 1, because of the smaller branching ratio into two photons (39%) and the small $\eta/\pi^0 \approx 0.5$ production ratio. The raw yields become comparable only around 20 GeV/c. Therefore we applied an $\alpha < 0.6$ photon pair energy asymmetry cut (as opposed to $\alpha < 0.8$ for π^0) in order to improve the signal-to-background ratio in the η region. The other part of the η analysis is the same as the one described in [11,15].

The raw η yield is always counted by integrating the histogram bin content in the η mass window (typically ± 30 MeV/c^2), but the way we treat the underlying combinatorial background varies as a function of p_T. In Au + Au up to 10 GeV/c, mixed event subtraction is used. The η region is then fitted with a polynomial and Gaussian (see inset in Fig. 1) to estimate the residual background. When the signal-to-background ratio reaches 1.0, already in the 7–10 GeV/c range, depending on centrality, mixed event subtraction is no longer needed; a polynomial and Gaussian fit is used on the original invariant mass distribution to estimate the background. At even higher p_T (12–16 GeV/c) we estimate the residual background under the peak simply from the average bin content of the sidebands (the regions above and below the peak).

TABLE I. Typical systematic uncertainties on η spectra and R_{AA}. See text for explanation of error types.

Source	Type	Au + Au	$p + p$	R_{AA}
Raw yield	B	7%	3%	6.3%
Acceptance variations	B	1.5%	1.5%	2.1%
Photon PID	B	3%	3%	3%
Acceptance × efficiency	A	3%	3%	4.2%
Energy scale	B	8%	8%	11.3%
Conversion (HBD)	C	1.3%	N/A	1.3%
Conversion (other)	C	5%	5%	N/A
BBC cross section	C	N/A	9.7%	9.7%
BBC efficiency	C	N/A	3.8%	3.8%
ERT norm.	C	N/A	6.2%	6.2%

Systematic uncertainties are classified into three types: Type A is p_T uncorrelated ("point-by-point") and, for the purposes of fitting and plotting, is added in quadrature to the statistical errors. Type C is the overall normalization uncertainty allowing all points to move by the same fraction up or down. Type B is all other p_T-correlated uncertainties (including the cases where the shape of the correlation function is not known). Table I lists typical uncertainties on the spectra and R_{AA}. "Conversion (HBD)" stands for loss due to photon conversion in the Hadron Blind Detector, which was present in one of the two central arms during the 2007 (Au + Au) data taking. "ERT norm." stands for the normalization uncertainty of the EMCal–Ring-Imaging-Čerenkov trigger, selecting high-p_T photons and electrons. "Acceptance variations" are small day-by-day changes of dead areas in the detector and thus are independent for the $p + p$ and Au + Au runs. The systematic uncertainties on raw yield, photon particle identification (PID), and conversion (other) are common in $p + p$ and Au + Au, and hence were partially canceled out in the R_{AA} calculation.

Cross sections for $p + p \rightarrow \eta + X$ and invariant yield of inclusive η production in Au + Au collisions for different centralities are shown in Fig. 2. They cover the $5 < p_T < 22$ GeV/c range and five orders of magnitude in cross section

TABLE II. Parameters of the power-law fits A/p_T^n for Au + Au and $p + p$. The errors used for fit are the statistical and p_T-uncorrelated (type A) systematic uncertainties added in quadrature. The p_T range of the fits is 5–22 GeV/c.

System/Centrality	A	n	χ^2/NDF
Au + Au 0–5%	27.2 ± 11.9	7.90 ± 0.22	3.1/7
Au + Au 0–10%	17.6 ± 5.5	7.77 ± 0.15	10.6/8
Au + Au 10–20%	19.1 ± 5.9	7.89 ± 0.16	10.2/9
Au + Au 0–20%	18.5 ± 4.3	7.84 ± 0.12	10.5/7
Au + Au 20–40%	17.3 ± 4.2	8.01 ± 0.12	17.2/8
Au + Au 40–60%	9.53 ± 2.65	8.05 ± 0.15	5.5/8
Au + Au 20–60%	14.5 ± 2.5	8.07 ± 0.08	11.2/9
Au + Au 60–92%	1.13 ± 0.40	7.78 ± 0.18	2.98/6
Au + Au MinBias	10.4 ± 1.4	8.04 ± 0.08	9.41/9
$p + p$	8.84 ± 0.99	8.21 ± 0.05	8.33/9

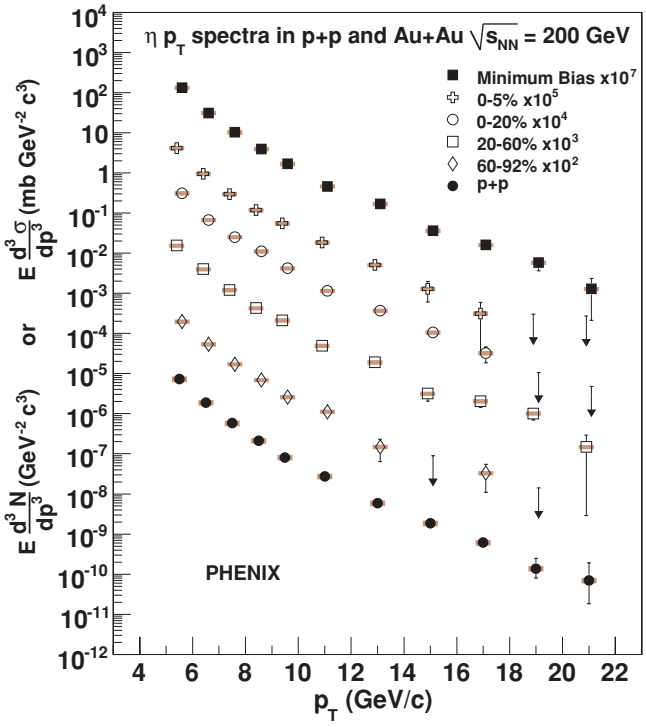

FIG. 2. (Color online) Cross section of $p + p \rightarrow \eta + X$ from the 2006 $p + p$ data set (solid circles) and η invariant yield in Au + Au collisions of various centralities (open symbols) and minimum bias (solid squares) from the 2007 data set. $p + p$ is shown at the true p_T value; all other spectra are shifted alternately by ± 0.1 GeV/c for better visibility of the error bars and upper limits.

(invariant yield). The overall normalization uncertainties (type C) are 13% for $p + p$ and 5% for Au + Au. Parameters of simple power-law fits (A/p_T^n) to various, partially overlapping centrality selections, including ones not shown in Fig. 2, are given in Table II. Fits include all available points in the $5 < p_T < 22$ GeV/c range but exclude upper limits. Only statistical and p_T-uncorrelated uncertainties were used in the fits. Note that for π^0 in Au + Au collisions the power n was consistent within uncertainties at all centralities [2] ranging from 8.00 ± 0.12 in 0–5% to 8.06 ± 0.08 in 80–92%, and for π^0 in $p + p$ the power n was 8.22 ± 0.09. In this measurement we find that for η production $p + p \rightarrow \eta + X$ the power n is the same as it was for π^0. The powers obtained for η in

TABLE III. Parameters from linear function fit to η $R_{\rm AA}$.

Centrality	$N_{\rm part}$	Slope	χ^2/NDF
0–5%	351	0.008 ± 0.008	2.77/7
0–10%	326	0.011 ± 0.007	9.79/7
10–20%	236	$0.010^{+0.009}_{-0.008}$	11.7/8
0–20%	280	$0.010^{+0.007}_{-0.006}$	10.8/7
20–40%	142	0.004 ± 0.010	15.7/8
40–60%	61.6	$0.010^{+0.018}_{-0.017}$	4.64/7
20–60%	102	0.005 ± 0.011	11.7/8
60–92%	11.8	$0.056^{+0.043}_{-0.038}$	1.52/6
MinBias	109	0.006 ± 0.007	10.1/8

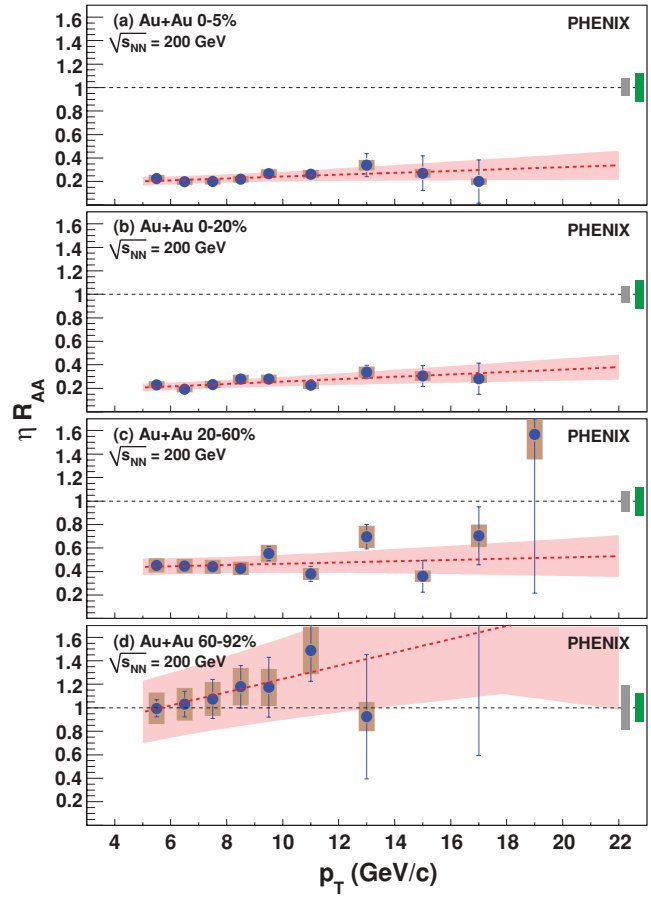

FIG. 3. (Color online) Nuclear modification factor for η at various centralities, calculated using the measured $p + p$ points. Dark (green) band around 1 indicates the absolute normalization error from $p + p$, light (gray) band is the (centrality-dependent) absolute normalization error from Au + Au. Error bars include statistical and p_T-uncorrelated systematic errors. Also shown: linear fits to the data with 1σ error bands.

Au + Au are also consistent with those from π^0 within two standard deviations.

The nuclear modification factor $R_{\rm AA}$ is defined as

$$R_{\rm AA} = \frac{1/N_{\rm evt} dN/dy\, dp_T}{\langle T_{\rm AB}\rangle d\sigma_{pp}/dy\, dp_T},$$

where σ_{pp} is the production cross section of the particle in $p + p$ collisions, and $\langle T_{\rm AB}\rangle$ is the nuclear thickness function averaged over a range of impact parameters for the given centrality, calculated within a Glauber model [13]. When calculating $R_{\rm AA}$, the measured $p + p$ points are used. $R_{\rm AA}$ for η production is shown in Fig. 3 for four centralities, along with linear fits to $R_{\rm AA}$ which properly take both systematic and statistical uncertainties into account. Fit parameters are listed in Table III. In the measured p_T range we observe strong suppression in all but the most peripheral collisions. As shown in Fig. 4, for the minimum bias case the suppression is quite comparable to the one observed for π^0, and above 13 GeV/c the (relative) systematic errors are smaller.

Based upon the most central (0–5%) collisions in [10], we found that the π^0 $R_{\rm AA}$ is consistent with a completely flat p_T

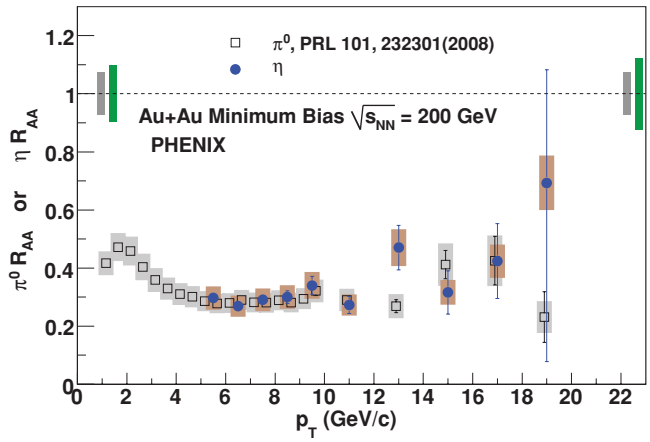

FIG. 4. (Color online) Nuclear modification factor $R_{\rm AA}$ for π^0 (open squares, points shifted for clarity, data from [2]) and η (solid circles, this analysis) in MB Au + Au collisions. Error bars include statistical and p_T-uncorrelated systematic errors, bands show p_T-correlated systematic errors. The pair of bands at $R_{\rm AA} = 1$ are the absolute normalization error for $p + p$ (larger, dark) and Au + Au (lighter) for π^0 (left) and η (right).

dependence when fitted in the $5 < p_T < 18$ GeV/c region, namely, the slope of a linear fit was $m = 0.0017^{+0.0035}_{-0.0039}$ c/GeV. Fitting the current η $R_{\rm AA}$ data with straight lines gives the slopes and uncertainties listed in Table III and shown in Fig. 5, where centrality is expressed in terms of participating nucleons $N_{\rm part}$. All slopes are consistent with zero; the largest deviation is less than 2σ (for the 0–20% centrality bin). One and two

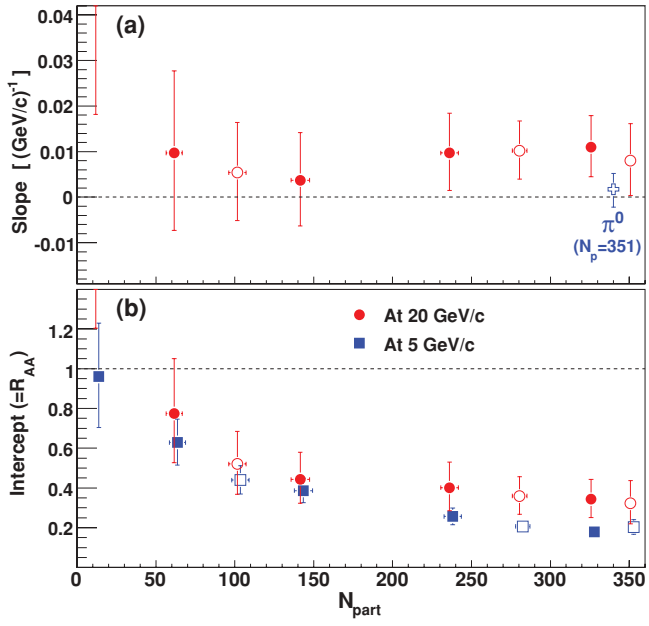

FIG. 5. (Color online) (a) Slopes of the linear fits (like the ones shown in Fig. 3) along with the fitting errors. Centrality is shown in terms of participating nucleons $N_{\rm part}$. Open symbols are overlapping, solid symbols are non-overlapping centrality bins (0–10%, 10–20%, 20–40%, 40–60%, and 60–92%). Also shown: slope of the linear fit to 0–5% π^0 data [10], shifted for better visibility. (b) Value of $R_{\rm AA}$ calculated from the fit at 5 GeV/c (blue) and 20 GeV/c (red).

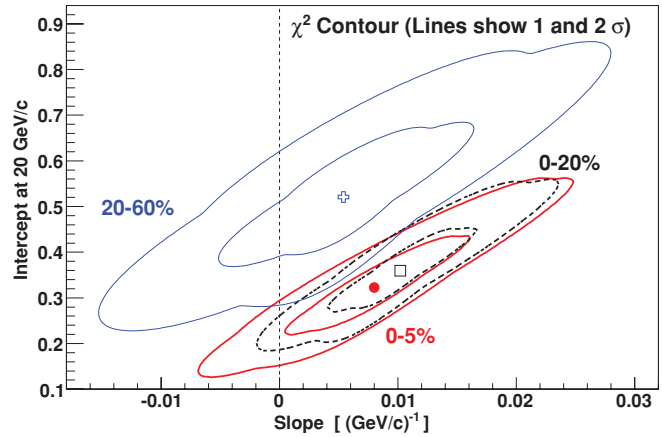

FIG. 6. (Color online) One and two standard deviation χ^2 contours of the linear fits to $R_{\rm AA}$ in Au + Au collisions for 0–5%, 0–20%, and 20–60% centralities.

standard deviation χ^2 contours for selected centrality bins are shown in Fig. 6. For 0–5% centrality we repeated the linear fits using only the first 3, 4, ..., $(n-1)$ points and found that the slope already stabilizes around its final value with the first few points; data above 10 GeV/c improve the significance but barely change the central value itself. The same is true for other centralities.

While the above result indicates that $R_{\rm AA}$ for η is consistent with a p_T-independent, constant value, and disfavors a *decreasing* $R_{\rm AA}$, a slow rise ($\sim$0.01c/GeV) of $R_{\rm AA}$ with increasing p_T cannot be excluded. In fact, a detailed statistical analysis, comparing to various theories, like the study done for π^0 in [10], is necessary once theoretical calculations of η production are available. However, *assuming* the linear dependence, we can calculate the $R_{\rm AA}$ values at 5 GeV/c (where the suppression is already at its maximum) and 20 GeV/c; the results are shown in the bottom panel of Fig. 5.

In summary, we measured invariant yields of η in $\sqrt{s_{NN}} =$ 200 GeV Au + Au collisions at various centralities, as well as the η production cross section in $\sqrt{s} = 200$ GeV $p + p$ collisions in the $5 < p_T < 22$ GeV/c transverse momentum range using the PbSc calorimeter of the PHENIX experiment at RHIC. The nuclear modification factor for η in minimum bias collisions is consistent with earlier π^0 results. In conclusion, linear fits to $R_{\rm AA}$ as a function of p_T indicate that $R_{\rm AA}$ is consistent with a constant at all centralities, although a slow rise cannot be excluded.

We thank the staff of the Collider-Accelerator and Physics Departments at BNL for their vital contributions. We acknowledge support from the Office of Nuclear Physics in DOE Office of Science, NSF, and a sponsored research grant from Renaissance Technologies (United States), MEXT and JSPS (Japan), CNPq and FAPESP (Brazil), NSFC (China), MSMT (Czech Republic), IN2P3/CNRS and CEA (France), BMBF, DAAD, and AvH (Germany), OTKA (Hungary), DAE and DST (India), ISF (Israel), NRF (Korea), MES, RAS, and FAAE (Russia), VR and KAW (Sweden), US CRDF for the FSU, US-Hungary Fulbright, and US-Israel BSF.

[1] K. Adcox *et al.*, Phys. Rev. Lett. **88**, 022301 (2001).
[2] A. Adare *et al.*, Phys. Rev. Lett. **101**, 232301 (2008).
[3] S. S. Adler *et al.*, Phys. Rev. Lett. **91**, 072303 (2003).
[4] S. A. Bass, C. Gale, A. Majumder, C. Nonaka, G.-Y. Qin, T. Renk, and J. Ruppert, Phys. Rev. C **79**, 024901 (2009).
[5] H. Liu, K. Rajagopal, and U. A. Wiedemann, Phys. Rev. Lett. **97**, 182301 (2006).
[6] W. A. Horowitz and M. Gyulassy, Phys. Lett. B **666**, 320 (2008).
[7] P. M. Chesler, K. Jensen, A. Karch, and L. G. Yaffe, Phys. Rev. D **79**, 125015 (2009).
[8] S. S. Gubser, D. R. Gulotta, S. S. Pufu, and F. D. Rocha, J. High Energy Phys. 10 (2008) 052.
[9] D. E. Kharzeev, arXiv:0806.0358 [nucl-th].
[10] A. Adare *et al.*, Phys. Rev. C **77**, 064907 (2008).
[11] S. S. Adler *et al.*, Phys. Rev. C **75**, 024909 (2007).
[12] M. Allen *et al.*, Nucl. Instrum. Methods Phys. Res. A **499**, 549 (2003).
[13] M. L. Miller, K. Reygers, S. J. Sanders, and P. Steinberg, Annu. Rev. Nucl. Part. Sci. **57**, 205 (2007).
[14] L. Aphecetche *et al.*, Nucl. Instrum. Methods Phys. Res. A **499**, 521 (2003).
[15] S. S. Adler *et al.*, Phys. Rev. C **76**, 034904 (2007).